Nanomesh aluminum films for LC alignment. Theoretical and experimental modeling

A.K. Dadivanyan[1], V.V. Belyaev[1,3], D.N. Chausov[1], A.A. Stepanov[2], A.G. Smirnov[2], A.G. Tsybin[2] , M.A.Osipov [4]

Affiliations:

[1]Education & Research Lab of Theoretical and Applied Nanotechnology,

Moscow Region State University, Moscow, Russia

Tel. +7(495)5771981; fax: +7(499)2612228, e-mail: vic_belyaev@mail.ru

[2]Belarusian State University of Informatics and Radioelectronics, Belarus, Minsk, P. Browki str. 6, 220013

[3]Russian People Friendship University, Moscow, Russia

[4]Department of Mathematics and Statistics, University of Strathclyde, Glasgow, UK

*Corresponding author: V. Belyaev vic_belyaev@mail.ru

A. Smirnov smirnov@bsuir.by

A. Stsiapanau an.step.a@gmail.com

Keywords: liquid crystal alignment, micropores, anchoring

Abstract

Methods of fabrication of nanomesh aluminum films for LC alignment and their structure are described. A dependence of the pores' diameter *vs*. their fabrication conditions is found. A dependence of the alumina nanomesh on the pores' performances is simulated too.

A theory of LC alignment in such system is proposed that allows prediction of the alignment type and explain experimental data. The LC orientation type is determined by the free anchoring energy and the micropore diameter. The difference of both planar and homeotropic anchoring energy is lower than the interaction energy by two orders of magnitude.

(1) **Objective and Background**

An opportunity of LC alignment by substrates with porous surface has been demonstrated in [1-5]. There are high-purity aluminum layers subjected by anodic oxidation process and forming porous structure of aluminum oxide Al_2O_3. Besides of the LC alignment they can be used as transparent electrodes [2,6,7], antireflective coatings [8], light emitting devices [9]. The type of the LC orientation depends on the pores' size and LC anchoring [7,10].

Design and fabrication of LCD elements with nanomesh alumina structure are presented in [3,4,10,11].

In [7] optical properties and surface resistance have been simulated for nanomesh alumina films by using FDTD Solutions LUMERICAl and COMSOL Multiphysics software.

Theoretical modeling of the LC alignment on flat surfaces of carbon, polyethyleme and polyorganosiloxane has been developed in [12-14].

Type of the NLC alignment on the nanomesh alumina films is presented in Table 1 [8].

Pores diameter \ Anchoring energy (J/m^2)	50 nm	100 nm	150 nm	200 nm	250 nm
$1 \cdot 10^{-2}$	planar	planar	planar	planar	planar
$1 \cdot 10^{-4}$	vertical	vertical	tilted	tilted	planar
$1 \cdot 10^{-6}$	vertical	vertical	vertical	vertical	tilted

However the physical mechanism of this effect is not clear. The paper goal is a theoretical model of the effect for different pores.

(2) **Results**

2.1. Fabrication of nanomesh alumina films for LC alignment

We have selected the technology of electrochemical anodizing of thin aluminum films as the major technology of producing nanomesh aluminum films since it allows producing self-organizing hexagonal-packed nanostructures without using lithographic processes. The analysis of experimental results enables to determine the relationship between the cell size D_c of the nanomesh aluminum film and anodizing voltage U. Thus, if we measure and calculate average cell sizes of nanomesh aluminum films and associate them with corresponding voltages under which the nanomesh aluminum films are produced in different electrolytes, we will get a linear relationship which shows that the cell size D_c of the nanomesh aluminum films is directly proportional to the applied voltage $D_c = 2{,}5U$. The proportional relationship between the cell size and anodizing voltage enables to control the morphology of the structure.

The analysis of experimental results reveals the opportunity to produce self-organizing nanomesh aluminum films with specific cell sizes D_c of 50–600 nm by means of controllable electrochemical anodizing of aluminum nanomesh with the thickness over 200 nm which is followed by selective etching of Al_2O_3.

2.2. Structure of nanomesh alumina films

Other characteristical parameters of a nanomesh aluminum film are the diameter of pores D_p, maximal thickness H_{max}, minimal thickness H_{min} and width L_{min} of the aluminum nanomesh (Figure 1). By controllable completion of anodizing after selective etching of porous oxide an aluminum film acquires nanomesh morphology with different fill factor f, that also characterizes the nanomesh film and is determined as the ratio (relation) of a pore area S_{Dp} to a cell area S_{Dc}.

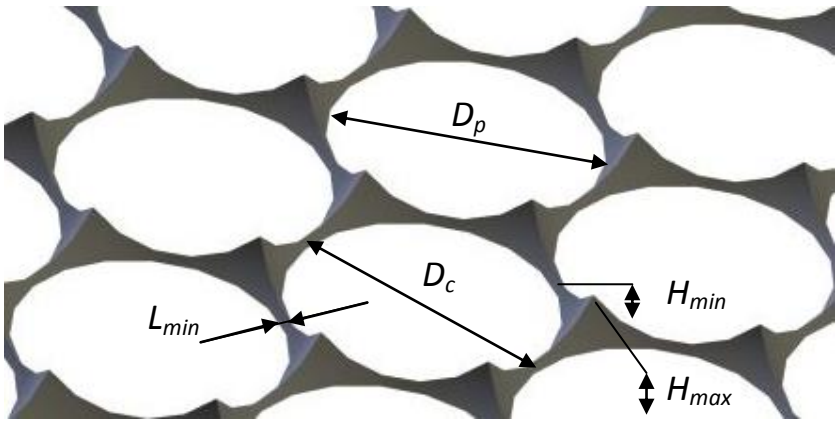

Figure 1 – Schematical image of morphology of a nanomesh aluminum film

To determine the relationship between characteristical parameters of the nanomesh aluminum film and the time of its formation we have preset its morphology by means of hollow hemispheres with dense hexagonal packaging which are located in the aluminum film. The thickness of the aluminum film equals to the radius of the hemisphere. Figure 1 shows a schematic image of morphology of the nanomesh film.

This model depicts an approximation of the structure "porous alumina - aluminum" at the moment when the barrier layer touches upon the substrate. The further anodizing process corresponds to the movement of hemispheres under their preset radius and distance between them.

It is known, that the reduction of the wall thickness of alumina relates to the electrical field which induces the ions located at the junction of pore boundaries. Based on this idea, the value of ratio of thickness of the oxide wall to thickness of the barrier layer estimated numerically which results in the relation:

$$R_b = \frac{2}{\sqrt{3}} r_c.$$

In support of this idea, we have assumed that the bottom of a unit cell of the nanomesh aluminum is shaped as the regular hexagon with a side equal to thickness of the barrier layer of porous alumina. It is evident, that R_b here is a radius of a circle circumscribed around the cell and there is the relation $D_c = \sqrt{3} R_b$ (Figure 2 *a*).

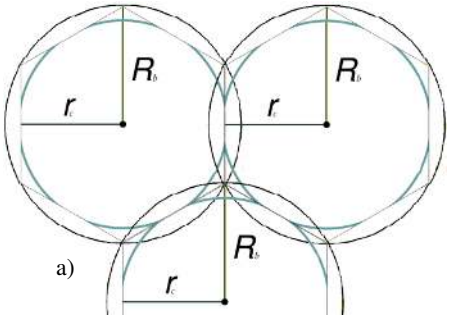

Fig. 2 – Schematical image of the unit cell of the nanomesh aluminum film (*a* – top view, *b* – cross sectional view)

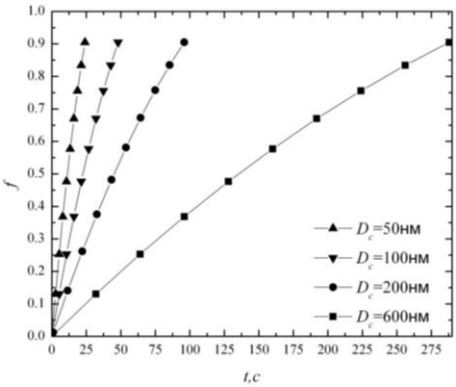

Fig. 3 – Relations between the fill factor *f* and the time of forming of nanomesh aluminum films with various cell sizes

As shown in Figure 2 *b*, at the moment when the bottom of the barrier layer touches upon the substrate it is possible to determine the maximal and minimal thickness of aluminum by corresponding relations:

$$H_{max0} = R_b = \frac{\sqrt{3}}{3} D_c,$$

$$H_{min0} = \frac{2}{\sqrt{3}} r_c - \sqrt{R_b^2 - r_c^2} = \frac{2}{\sqrt{3}} r_c - \sqrt{\frac{4}{3} r_c^2 - r_c^2} = \frac{\sqrt{3}}{6} D_c.$$

H_{max0} and H_{min0} will linearly decrease during growth of porous oxide down to $H_{min} = 0.$ Meanwhile, maximal thickness of aluminum H_{max} equals:

$$H_{max} = H_{min0} = \frac{\sqrt{3}}{6} D_c.$$

Pore diameter D_p, will increase alongside with the enlargement of the contact area between the substrate and the barrier layer of porous oxide, which depends on anodizing time *t*. Then D_p can be calculated by the following formula:

$$D_p(t) = 2\sqrt{\frac{1}{3} D_c^2 - \left(\frac{1}{\sqrt{3}} D_c - \Delta r(t)\right)^2},$$

where $\Delta r = vt$ is a downward shift of the barrier layer at speed *v* within the period of time *t* since contact with the substrate. Maximal value of the pore diameter equals to the cell size and is reached at the moment of breakdown under $\Delta r_{max} = H_{min0}$, with anodizing process ceasing at this very moment.

Width of the aluminum nanomesh in the narrowest place L_{min} is calculated by the formula:

$$L_{\min}(t) = D_c - D_p(t).$$

There is a practical necessity to determine the relationship between the fill factor *f* and the time of formation:

$$f = \frac{S_p(t)}{S_c} = \frac{\pi D_p^2(t)}{2\sqrt{3} D_c^2} = \frac{4\pi\left(\frac{1}{3} D_c^2 - \left(\frac{1}{\sqrt{3}} D_c - vt\right)^2\right)}{2\sqrt{3} D_c^2} = \frac{2\pi\left(\frac{2}{\sqrt{3}} D_c vt - v^2 t^2\right)}{\sqrt{3} D_c^2}$$

According to the obtained expression, maximal value of fill factor may reach 0.9 under $D_p = D_c$.

Using experimental data we have determined that the speed of aluminum film anodizing *v* equals to 0.6 μm/s under anodizing current density of 2 mA/cm^2.

To estimate the time of the aluminum nanomesh forming with the preset fill factor *f*, we have determined function relations *f(t)* for cell sizes D_c, equal to 50, 100, 200 and 600 nm correspondingly. Relations between fill factor *f* and the time of forming of nanomesh aluminum films with various cell sizes are shown in Figure 3.

Despite the quadratic time relation of fill factor *f*, it changes smoothly enough which enables to produce nanomesh aluminum films with the required fill factor.

It also follows from the obtained relations that the time of forming of nanomesh aluminum films ranges from 25 to 300 s and is determined by the cell size. This time range is adaptable to streamlined production and sufficient for controllable and reproducing production of nanomesh aluminum films with the preset fill factor.

2.3. Theory of LC alignment in micro- and nanopores' system

If anchoring energy is small ($\Delta G = 10^{-6}\, J * m^{-2}$) the LC alignment in the pores with diameter up to 200 nm is homeotropic (vertical). Experiments with analog models demonstrated the homeotropic type of the LC orientation if the LC does not interact with the micropore surface and the pore diameter is of order of the LC cluster size.

Therefore the maximum cluster diameter is approximately equal to 200 nm and the cluster comprises ~400 molecules in one dimension because the mesogenic molecule's diameter is ~0.5 nm. Assume that the cluster form ratio is the same as for the LC molecules, i.e. ~5, then the cluster length is ~1 μm and the cluster comprises $0.6*10^8$ mesogenic molecules. This number is by one or two orders higher than the molecules' number in the cluster obtained in investigation of photoalignment []. Therefore the cluster length is 300-400 nm, its diameter is 65-85 nm (1/3 of the pore diameter) and the clusters' packing in the pore is of hexagonal type.

Other experiments with analog models demonstrated the planar type of the LC orientation if the LC does not interact with the micropore surface and the pore diameter is by 1.5-2 times larger than the LC cluster size (~ 1 μm).

For higher anchoring energy value ($\Delta G = 10^{-2} J * m^{-2}$) the LC orientation in the micropores is planar and independent on their size, for intermediate ΔG values is homeotropic at moderate pore diameter (up to 150 nm), tilted at pores' diameter from 150 nm to 250 nm.

The alignment type is determined by the anchoring energy

$$G_{pl} = H_{pl} - TS_{pl}$$

$$G_{hom} = H_{hom} - TS_{hom}$$

where G_{pl} and G_{hom} is Gibbs free energy, H_{pl} and H_{hom} is enthalpy, S_{pl} and S_{hom} is entropy in the case of both planar and homeotropic alignment, accordingly.

$$\Delta G = G_{pl} - G_{hom} = H_{pl} - H_{hom} - T(S_{pl} - S_{hom})$$

For $\Delta G < 0$ the orientation is planar, and $\Delta G < 0$ the orientation is homeotropic. For small anchoring energy $H_{pl} \approx H_{hom}$ and the orientation type is determined by the orientation entropy. If $S_{pl} > S_{hom}$ the orientation is planar, and $S_{pl} < S_{hom}$ the orientation is homeotropic. For both high and moderate anchoring energy the orientation type is determined by the orientation entropy because the difference of the energy of the LC interaction with the pore surface for both planar and hometropic orientation differs on the interaction of that molecules which touch the internal pore surface only. This difference is of order of 1/100 of the total interaction molecules-surface energy. If such difference was higher this effect resulted in the homeotropic orientation.

The entropy can be calculated by using the lattice model. The clusters are oriented independently and entropy is to find by using the Boltzmann formula:

$$S = k \ln W$$

where *k* is Boltzmann constant, and *W* is microstates number that correspond to the given macrostate.

The microstates number in the case of the planar orientation is equal to:

$$W_{pl} = \frac{(\nu\nu_0^{pl})!}{(\nu\nu_0^{pl} - N)!\,N!},$$

where *N* is the mole clusters number ($N=N_a/n$),

n is the mesogen molecules number in the cluster,

ν is the micropores number in one mole,

ν_0^{pl} is the number of the orienational states in the pore in the case of the planar orientation.

In the case of the homeotropic orientation the placement number is equal to:

$$W_{hom} = \frac{(\nu\nu_0^{hom})!}{(\nu\nu_0^{hom} - N)!\,N!},$$

where ν_0^{hom} is the number of the orienational states in the pore in the case of the homeotropic orientation.

The molar entropy difference for both planar and homeotropic orientation is equal to

$$\Delta S = S_{pl.} - S_{hom.} = k\,ln\frac{(\nu\nu_0^{pl})!\,(\nu\nu_0^{hom} - N)!}{(\nu\nu_0^{hom})!\,(\nu\nu_0^{pl} - N)!}$$

One can obtain by using the Stirling formula and the expansion $ln(1 \pm x) = \pm x - \frac{x^2}{2} \pm \pm \frac{x^3}{3}$:

$$\Delta S = k\left[N ln\frac{\nu_0^{pl}}{\nu_0^{hom}} - \frac{N^2}{2}\left(\frac{1}{\nu\nu_0^{pl}} - \frac{1}{\nu\nu_0^{hom}}\right) - \frac{N^3}{3}\left(\frac{1}{(\nu\nu_0^{pl})^2} - \frac{1}{(\nu\nu_0^{hom})^2}\right)\right]$$

The cells' number in one micropore is equal to ν_{pl} and ν_{hom} for both planar and homeotropic orientation, accordingly. $\nu_{pl} = \nu_0^{pl} \cdot \nu$ and $\nu_{hom} = \nu_0^{hom} \cdot \nu$, where ν – is the micropores' number per one mesogen mole, ν_0^{pl} and ν_0^{hom} are the cells' number in one micropore for both planar and homeotropic orientation, accordingly, i.e. the number of possible cluster orientations in the micropore. It is to assume $\nu_0^{pl} = \nu_0^{hom} = \nu_0$, then $\nu_{pl} = \nu_0 \cdot \nu$ and $\nu_{hom} = \nu_0 \cdot \nu$.

For both planar and homeotropic orientation the numbers the clusters orientation combinations in one mesogen mole, accordingly, W_{pl} and W_{hom} are equal to:

$$W_{pl} = \frac{\nu_{pl}!}{(2N)!(\nu_{pl} - 2N)!} = \frac{(\nu \cdot \nu_0)!}{(2N)!\,(\nu \cdot \nu_0 - 2N)!}$$

$$W_{hom} = \frac{\nu_{hom}!}{(n_0N)!(\nu_{hom} - n_0N)!} = \frac{(\nu \cdot \nu_0)!}{(n_0N)!\,(\nu \cdot \nu_0 - n_0N)!}$$

If exclude the same states in W_{pl} expression 2*N* is to use instead of *N*; for W_{hom} is to use $n_0 N$, where n_0 is maximum number of the mesogen molecules in outer cluster's layer in the plane perpendicular to the cluster symmetry axis. The value of n_0 is equal to $n_0 = \frac{\pi D}{d}$, where *D* is the cluster diameter (~200 nm), *d* diameter of the mesogen molecule (0.5 nm); therefore $n = 400\,\pi$.

The entropy difference is equal to:

$$\Delta S = S^{pl} - S^{hom} = k\,ln\frac{W_{pl}}{W_{hom}} = k\,ln\frac{(n_0N)!(v\cdot v_0 - n_0N)!}{(2N)!(v\cdot v_0 - 2N)!}$$

By using the Stirling formula one can obtain:

$$\Delta S = k\,ln\frac{W_{pl}}{W_{hom}} = -n_0N\,ln\frac{v\cdot v_0 - n_0N}{n_0N} - 2N\,ln\frac{v\cdot v_0 - 2N}{2N} - v\cdot v_0\,ln\frac{v\cdot v_0 - 2N}{v\cdot v_0 - n_0N}$$

The model presented in this part allows calculate the thermodynamic parameters that determine the LC alignment. For the clusters with diameter presented in Part 2.2 a part of the free anchoring energy difference that arises owing to the difference of both planar and homeotropic orientation entropy is equal to $(0.3 \div 3)\times10^{-5}$ J/m^2. It corresponds well to low magnitude of the free anchoring energy presented in Table 1.

Conclusion

1. A dependence of the pores' diameter *vs*. their fabrication conditions is found.
2. A dependence of the minimum width of the alumina nanomesh on the pores' performances is simulated too.
3. The LC orientation type is determined by the LC clusters formation and their size in relation to the pore size.
4. The mesogen orientation is determined the entropy difference for both planar and homeotropic orientation.

(3) **Impact**

Simple methods of fabrication of nanomesh alumina films for LC alignment are presented. At first time modeling of their structure and manufacturing process is described. Advantages of such films are easy fabrication, stability to ambient conditions, opportunity of controlling the LC orientation type.

At first time the theory of LC alignment in such system is proposed that allows prediction of the alignment type and explain experimental data.

(4) References

1. A. Smirnov, A. Stsiapanau, A. Mohammed, E. Mukha, H. S. Kwok, A. Murauski, "Combined nanostructured layers for display applications", Proc. SID Symposium "Display Week-2011", pp. 1385–1387, Los Angeles, CA, May 2011.
2. V. Bezborodov, S. Mikhalyonok, I. Zharski, O. Dormeshkin, A. Smirnov and A. Stsiapanau, "New Concept for the Design, Synthesis, and Application of Nanostructured Anisotropic Materials and Conductive and Alignment Coatings for High-Efficient Displays and Photonic Devices", 33rd International Display Research Conference EuroDisplay 2013, London, UK. 16-19 September 2013. Conference Proceedings. P.81-84.
3. S.K. Lazarouk, D.A. Sasinovich, P.S. Katsuba, A.G. Smirnov, V.M. Astafjev, "LC alignment using nanostructured porous alumina", Proc. EuroDispla'2007, Moscow, Russia, 14-18 September 2007.
4. S. Lazarouk, Anatoli Muravski, Dmitri Sashinovich, Vladimir Chigrinov, and Hoi Sing Kwok, Porous and Pillar Structures Formed by Anodization for Vertical Alignment of Nematic Liquid Crystal, Jpn. J. Appl. Phys., 46, No.10A, pp. 6889-6892 (2007).
5. T. Maeda, and K. Hiroshima, Japanese Journal of Applied Physics, Vol. 43, No. 8A, 2004, p. L 1004–L 1006.
6. A. Smirnov, A. Stsiapanau, Y. Mukha, V. Mazaeva, V. Belyaev, "Transparent conductive coatings made by electrochemical and physicochemical methods", SID'13 Digest.
7. A. Stsiapanau, A. Smirnov, A. Yasyunas et al., „Simulation of structure and electro-physical properties of nanomesh alumina films", 20th Advanced Display and Lighting Technologies Symposium, Yalta, Ukraine, 8-12 October 2012, Abstracts, p.37.
8. A. Smirnov, A. Stsiapanau, E. Mukha,, "Nanomesh antireflective coatings for silicon solar batteries with Schottky structure", 20th Advanced Display and Lighting Technologies Symposium, Yalta, Ukraine, 8-12 October 2012, Abstracts, p.22.
9. A. Smirnov, P. Poznyak, A. Stsiapanau, et al., „Mechanism of light emission in LED on the base of nanoporous silicon", 20th Advanced Display and Lighting Technologies Symposium, Yalta, Ukraine, 8-12 October 2012, Abstracts, p.8.
10. A. Stsiapanau, A. Smirnov, Y. Satskevich et al., „Design and fabrication of LCD elements with Nanomesh alumina structure", 20th Advanced Display and Lighting Technologies Symposium, Yalta, Ukraine, 8-12 October 2012, Abstracts, p.7.
11. A. Stsiapanau, A. Smirnov, V. Astafyev et al., "Formation methods of regular surface structures", 20th Advanced Display and Lighting Technologies Symposium, Yalta, Ukraine, 8-12 October 2012, Abstracts, p.24.
12. A.K. Dadivanyan, Y. M. Pashinina, D.N. Chausov, V.V. Belyaev, and A.S. Solomatin, Orientation of mesogen and hydrocarbon molecules on graphite and polyethylene crystal surfaces // Molecular Crystals & Liquid Crystals, 2011, ISSN 1542-1406, V. 545, Issue 1, P. 159/[1383]-167/[1391].
13. A.K. Dadivanyan, O.V. Noah, Yu.M. Pashinina, V.V. Belyaev, V.G. Chigrinov, D.N. Chausov, Anchoring energy of liquid crystals // Molecular Crystals & Liquid Crystals, Philadelphia, USA, 2012, V. 560, Issue 1, P.108-114.
14. A. K. Dadivanyan, D. N. Chausov, O. V. Noa, V. V. Belyaev, V. G. Chigrinov, Yu. M. Pashinina, Influence of the order parameter on the anchoring energy of liquid crystals, Journal of Experimental and Theoretical Physics, V.115, No. 6, pp 1100-1104 (2012).

(5) **Prior Publications**

This paper continues our presentations [1,2,6]. The results obtained at present do not repeat the results presented earlier. The theory is absolutely new. The simulation results have not been published anywhere.